

Inverse Aggregation Behavior of Alkali-Metal Triazenides

Hyui Sul Lee and Mark Niemeyer*

Institut für Anorganische Chemie, Universität Stuttgart,
Pfaffenwaldring 55, 70569 Stuttgart, Germany

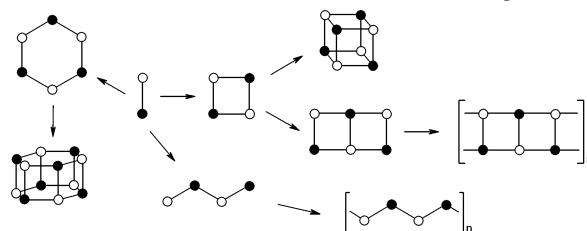
Received May 19, 2006

Higher aggregated alkali-metal compounds are usually obtained with increasing radius of the metal. Alkali-metal salts derived from the sterically crowded triazenido ligand $\text{Tph}_2\text{N}_3\text{H}$ [$\text{Tph} = \text{C}_6\text{H}_3\text{-}2,6\text{-(C}_6\text{H}_2\text{-}2,4,6\text{-i-Pr}_3)_2$] do not obey this principle. Interestingly, these compounds show *inverse aggregation* behavior in the solid state: the potassium and cesium salts crystallize as discrete *monomers* in which the cations interact with flanking arene rings of the diaryltriazenido ligands, whereas the lithium derivative is *dimeric* with a more conventional heteroatom-bridged structure.

Alkali-metal salts of organo-substituted group 14–16 elements, in particular the lithium, sodium, and potassium derivatives, are key reagents in organometallic synthesis and coordination chemistry.¹ Understanding the structure and aggregation of these compounds is therefore of fundamental interest to rationalize their different properties and reactivity. The degree of aggregation n for $(\text{MER}_x)_n$ compounds [$\text{M} =$ alkali metal, $\text{E} =$ group 14 ($x = 3$), 15 ($x = 2$), and 16 ($x = 1$) elements] depends on the nature of the metal (ionic radius and polarizability), steric demand and hapticity of the substituents, and donor solvation of the metal atom. Moreover, the avoidance of coordinating solvents often leads to novel structures and unusual metal–ligand interactions. Examples of the latter include agostic-type interactions with alkyl-substituted ligands or metal– π -arene interactions in aryl-substituted ligand systems. The pronounced tendency of the electron-deficient alkali-metal complexes^{1,2} or organyls³ to form aggregates in the absence of coordinating solvents or additional σ -donor atoms is reflected by the large number of structurally characterized oligo- and polymeric compounds, with the most common structural motives depicted in Scheme 1. In contrast, few structures of monomeric solvent-free compounds containing mono- and bidentate ligands have been reported.⁴

* To whom correspondence should be addressed. E-mail: mn@lanth.de.

- (1) Hanusa, T. P. In *Comprehensive Coordination Chemistry II*; McCleverty, J. A., Meyer, T. J., Eds.; Elsevier: Oxford, U.K., 2004; Vol. 3, Chapter 1, p 1.
- (2) Weiss, E. *Angew. Chem.* **1993**, *105*, 1565; *Angew. Chem., Int. Ed.* **1993**, *32*, 1501.
- (3) (a) Setzer, W. N.; Schleyer, P. v. R. *Adv. Organomet. Chem.* **1985**, *24*, 354. (b) Schade, C.; Schleyer, P. v. R. *Adv. Organomet. Chem.* **1987**, *27*, 169. (c) Smith, J. D. *Adv. Organomet. Chem.* **1999**, *43*, 354.

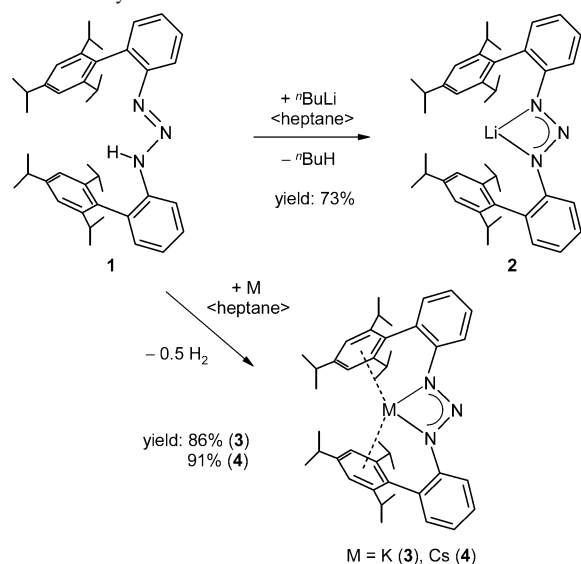
Scheme 1. Common Structural Motifs for $(\text{MER}_x)_n$ Compounds

In homoleptic complexes, higher aggregated derivatives are normally obtained with increasing radius of the alkali-metal cation.⁵ In this Communication, we describe the preparation and characterization of alkane-soluble alkali-metal salts of a novel sterically crowded triazenido ligand that do not obey this principle. Interestingly, these compounds show *inverse aggregation* behavior in the solid state: the cesium and potassium derivatives crystallize as discrete *monomers*, whereas the lithium salt is *dimeric*.

We recently succeeded in the preparation of derivatives of aryl-substituted, sterically crowded triazenido ligands, including the first examples of structurally characterized aryl compounds of the heavier alkaline-earth metals calcium, strontium, and barium⁶ and unsolvated pentafluorophenyl organyls of the divalent lanthanides ytterbium and europium.⁷ Because these novel triazenido groups may also find applications as ancillary ligands in catalysis, we have now prepared several alkali-metal derivatives to use them as transfer reagents. The alkali-metal triazenides are accessible in heptane as the solvent via metalation of the triazene $\text{Tph}_2\text{N}_3\text{H}$ (**1**; $\text{Tph} = 2\text{-TripC}_6\text{H}_4$ with $\text{Trip} = 2,4,6\text{-i-Pr}_3\text{C}_6\text{H}_2$) with either n -butyllithium or alkali metal (Scheme 2).⁸ After crystallization, the solvent-free compounds $[\text{M}(\text{N}_3\text{Tph}_2)]$

- (4) The known examples are restricted to some Li compounds: (a) the silyl and germyl $[\text{LiE}(\text{SiMe}_t\text{Bu}_{2-t})_3]$ ($\text{E} = \text{Si, Ge}$) (Nakamoto, M.; Fukawa, T.; Lee, V. Y.; Sekiguchi, A. *J. Am. Chem. Soc.* **2002**, *124*, 15160); (b) the β -diketiminato $[\text{Li}\{\text{TbtNC}(\text{Me})\text{CHC}(\text{Me})\text{NMes}\}]$ ($\text{Tbt} = 2,4,6\text{-[CH}(\text{SiMe}_3)_2\text{]}_3\text{C}_6\text{H}_2$, $\text{Mes} = \text{mesityl}$) (Takeda, N.; Hamaki, H.; Tokitoh, N. *Chem. Lett.* **2004**, *33*, 134).
- (5) Using very bulky ligands, it is possible on very rare occasions to stabilize the same degree of aggregation over the whole range of alkali metals. One elusive example for monodentate ligands is a series of dimeric metal thiophenolates $[\text{MSC}_6\text{H}_3\text{Trip}_{2-2,6}]_2$ ($\text{M} = \text{Li, Na, K, Rb, Cs}$): Niemeyer, M.; Power, P. P. *Inorg. Chem.* **1996**, *35*, 7264.
- (6) Hauber, S.-O.; Lissner, F.; Deacon, G. B.; Niemeyer, M. *Angew. Chem.* **2005**, *117*, 6021; *Angew. Chem., Int. Ed.* **2005**, *44*, 5871.
- (7) Hauber, S.-O.; Niemeyer, M. *Inorg. Chem.* **2005**, *44*, 8644.

Scheme 2. Synthesis of 2–4



[M = Li (**2**), K (**3**), Cs (**4**)] are isolated in good to excellent yields. The deep-yellow or orange complexes show considerable thermal stability but decompose with N_2 evolution above 176 °C (**2**), 326 °C (**3**), or 340 °C (**4**). They are moisture-sensitive and possess good or moderate solubility in aromatic or aliphatic hydrocarbons. The IR spectra show strong ν_{as} N_3 absorptions in the range 1229–1262 cm^{-1} , which is indicative of the triazenido groups acting as chelating ligands.⁹

(8) Important spectroscopic and analytical data for **2–4** (synthetic procedures, IR data, and information about the synthesis and characterization of **1** are given in the Supporting Information). [LiN_3Tph_2] (**2**): mp 176–235 °C (color change to orange and red and decomposition to a brown-red liquid); ^1H NMR (400.1 MHz, benzene- d_6) δ 1.08 + 1.09 (2 \times d, $^3J_{\text{HH}} = 6.8$ Hz, 12H, *o*-CH(CH_3)₂), 1.24 (d, $^3J_{\text{HH}} = 6.8$ Hz, 12H, *p*-CH(CH_3)₂), 2.78 (sep, $^3J_{\text{HH}} = 6.8$ Hz, 4H, *o*-CH(CH_3)₂), 2.84 (sep, $^3J_{\text{HH}} = 6.8$ Hz, 2H, *p*-CH(CH_3)₂), 6.60 (d br, 2H, 6- C_6H_4), 6.88 (t, $^3J_{\text{HH}} = 7.3$ Hz, 2H, 4- C_6H_4), 6.92 (d, $^3J_{\text{HH}} = 7.3$ Hz, 2H, 3- C_6H_4), 7.14 (t, 2H, 5- C_6H_4), 7.17 (s, 4H, *m*-Trip); ^{13}C NMR (100.6 MHz, benzene- d_6) δ 23.9 + 24.2 (2 \times *o*-CH(CH_3)₂), 25.3 (*p*-CH(CH_3)₂), 30.8 (*o*-CH(CH_3)₂), 34.5 (*p*-CH(CH_3)₂), 120.8 (6- C_6H_4), 121.8 (*m*-Trip), 122.4 (4- C_6H_4), 127.9 (5- C_6H_4), 132.4 (3- C_6H_4), 130.0 (2- C_6H_4), 137.2 (*i*-Trip), 146.5 (*o*-Trip), 148.2 (*p*-Trip), 150.4 (1- C_6H_4); ^7Li NMR (155.5 MHz, benzene- d_6) δ -0.11. Anal. Calcd for $\text{C}_{42}\text{H}_{54}\text{LiN}_3$: C, 82.99; H, 8.96; N, 6.91. Found: C, 83.37; H, 8.93; N, 6.95. [KN_3Tph_2] (**3**): mp 326–332 °C (minor dec); ^1H NMR (250.1 MHz, benzene- d_6) δ 0.82 + 1.07 (2 \times d, $^3J_{\text{HH}} = 6.9$ Hz, 12H, *o*-CH(CH_3)₂), 1.05 (d, $^3J_{\text{HH}} = 6.9$ Hz, 12H, *p*-CH(CH_3)₂), 2.62 (sep, $^3J_{\text{HH}} = 6.9$ Hz, 2H, *p*-CH(CH_3)₂), 3.03 (sep, $^3J_{\text{HH}} = 6.9$ Hz, 4H, *o*-CH(CH_3)₂), 6.89 (s, 4H, *m*-Trip), 7.02 (t, $^3J_{\text{HH}} = 7.3$ Hz, 2H, 4- C_6H_4), 7.16 (d, 2H, 3- C_6H_4), 7.39 (t, $^3J_{\text{HH}} = 7.3$ Hz, 2H, 5- C_6H_4), 8.38 (d, $^3J_{\text{HH}} = 7.3$ Hz, 2H, 6- C_6H_4); ^{13}C NMR (62.9 MHz, benzene- d_6) δ 23.9 + 24.2 (2 \times *o*-CH(CH_3)₂), 24.5 (*p*-CH(CH_3)₂), 30.6 (*o*-CH(CH_3)₂), 34.1 (*p*-CH(CH_3)₂), 114.8 (6- C_6H_4), 119.5 (*m*-Trip), 120.5 (4- C_6H_4), 128.9 (5- C_6H_4), 129.3 (3- C_6H_4), 130.7 (2- C_6H_4), 140.9 (*i*-Trip), 147.4 (*p*-Trip), 148.9 (*o*-Trip), 153.2 (1- C_6H_4); EI MS (70 eV) m/z (%) 639.4 (100) [M^+], 573.4 (2) [Tph_2NH] $^+$. Anal. Calcd for $\text{C}_{42}\text{H}_{54}\text{KN}_3$: C, 78.82; H, 8.50; N, 6.57. Found: C, 78.20; H, 8.48; N, 6.58. [CsN_3Tph_2] (**4**): mp 340–358 °C (minor dec); ^1H NMR (250.1 MHz, benzene- d_6) δ 0.88 + 1.08 (2 \times d, $^3J_{\text{HH}} = 6.9$ Hz, 12H, *o*-CH(CH_3)₂), 1.01 (d, $^3J_{\text{HH}} = 6.9$ Hz, 12H, *p*-CH(CH_3)₂), 2.59 (sep, $^3J_{\text{HH}} = 6.9$ Hz, 2H, *p*-CH(CH_3)₂), 3.10 (sep, $^3J_{\text{HH}} = 6.9$ Hz, 4H, *o*-CH(CH_3)₂), 6.88 (s, 4H, *m*-Trip), 7.01 (t, $^3J_{\text{HH}} = 7.3$ Hz, 2H, 4- C_6H_4), 7.12 (d, 2H, 3- C_6H_4), 7.40 (t, $^3J_{\text{HH}} = 7.6$ Hz, 2H, 5- C_6H_4), 8.47 (d, $^3J_{\text{HH}} = 7.6$ Hz, 2H, 6- C_6H_4); ^{13}C NMR (62.9 MHz, benzene- d_6) δ 23.9 + 24.1 (2 \times *o*-CH(CH_3)₂), 24.6 (*p*-CH(CH_3)₂), 30.7 (*o*-CH(CH_3)₂), 34.4 (*p*-CH(CH_3)₂), 115.2 (6- C_6H_4), 120.4 (*m*-Trip), 120.4 (4- C_6H_4), 128.8 (5- C_6H_4), 129.6 (3- C_6H_4), 130.5 (2- C_6H_4), 141.8 (*i*-Trip), 147.4 (*p*-Trip), 148.6 (*o*-Trip), 154.6 (1- C_6H_4). Anal. Calcd for $\text{C}_{42}\text{H}_{54}\text{CsN}_3$: C, 68.74; H, 7.42; N, 5.73. Found: C, 68.72; H, 7.41; N, 5.73.

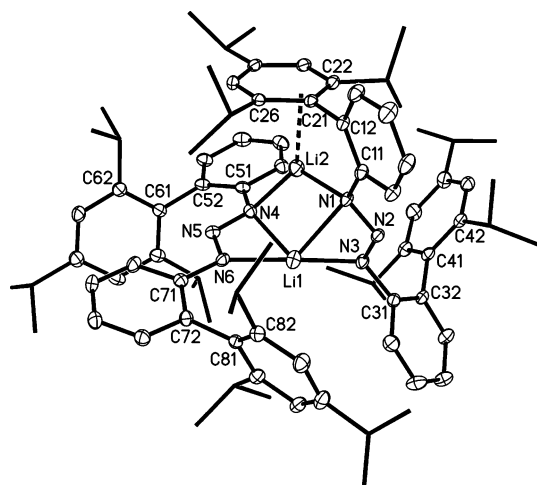


Figure 1. Molecular structure of (**2**)₂ with thermal ellipsoids set to 30% probability. Hydrogen atoms have been omitted, and carbon atoms of isopropyl groups are shown as lines for clarity. Selected bond lengths (Å), angles (deg), and dihedral angles (deg): Li1–N1 = 2.389(9), Li1–N3 = 1.960(8), Li1–N4 = 2.234(9), Li1–N6 = 1.984(8), Li2–N1 = 2.013(7), Li2–N4 = 2.044(7), Li2⋯C21 = 2.343(7), Li2⋯C22 = 2.585(7), Li2⋯C26 = 2.605(7), N1–N2 = 1.339(3), N2–N3 = 1.296(4), N4–N5 = 1.317(4), N5–N6 = 1.304(4), N3–Li1–N6 = 176.9(6), N2–N1–C11–C16 = -23.6(4), N2–N3–C31–C36 = 82.0(4), N5–N4–C51–C56 = 179.5(3), N5–N6–C71–C76 = -10.5(5).

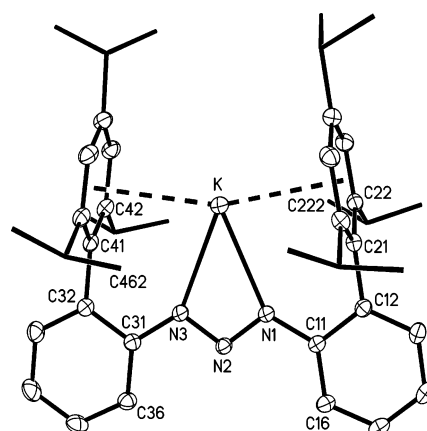


Figure 2. Molecular structure of **3** with thermal ellipsoids set to 30% probability. Hydrogen atoms have been omitted, and carbon atoms of isopropyl groups are shown as lines for clarity. Selected bond lengths (Å), angles (deg), and dihedral angles (deg) for **3** and **4** (in brackets): M–N1 = 2.7093(14) {3.065(5)}, M–N3 = 2.7232(14) {3.071(4)}, M⋯C21 = 3.3166(16) {3.680(5)}, M⋯C22 = 3.3472(16) {3.569(6)}, M⋯C23 = 3.3636(17) {3.541(6)}, M⋯C24 = 3.3689(17) {3.656(6)}, M⋯C25 = 3.3074(18) {3.741(6)}, M⋯C26 = 3.2948(17) {3.767(6)}, M⋯C41 = 3.3583(16) {3.699(5)}, M⋯C42 = 3.4435(17) {3.730(5)}, M⋯C43 = 3.4759(18) {3.756(6)}, M⋯C44 = 3.4482(18) {3.736(6)}, M⋯C45 = 3.3359(18) {3.664(6)}, M⋯C46 = 3.3060(17) {3.657(6)}, K⋯X6 = 3.027, {Cs⋯X5 = 3.367}, K⋯X5' = 3.087, {Cs⋯X5' = 3.430}, N1–N2 = 1.3016(18) {1.314(6)}, N2–N3 = 1.3086(17) {1.307(6)}, X6⋯K⋯X5' = 161.4, {X5⋯Cs⋯X5' = 169.6}, N2⋯K⋯X6 = 100.5, N2⋯K⋯X5' = 97.9 {N2⋯Cs⋯X5 = 93.5, N2⋯Cs⋯X5' = 88.3}, N2–N1–C11–C16 = 3.7(2) {3.2(9)}, N2–N3–C31–C36 = -4.4(2) {-2.0(9)}.

All compounds were examined by X-ray crystallography,¹⁰ and their molecular structures and important bond parameters are shown in Figures 1 and 2. Structurally characterized alkali-metal triazenides are scarce and have been limited so far to two solvated species with tolyl substituents, a dimeric lithium, and a polymeric potassium complex.¹¹

The lithium triazenide **2** crystallizes as a dimeric complex, in which $\mu_2:\eta^1, \eta^2$ -bound triazenido ligands bridge two lithium atoms. The cis arrangement of the triazenido ligands with

respect to the central, almost planar Li_2N_2 ring is quite unique and has no precedent in the structural chemistry of the related lithium amidinates.¹² One of the lithium atoms (Li1) shows a 2 + 2 coordination by four nitrogen atoms with two shorter [Li1–N3 1.960(8) Å; Li1–N6 1.984(8) Å] and two considerably longer [Li1–N4 2.234(9) Å; Li1–N1 2.389(9) Å] bonds. The other lithium atom (Li2) exhibits a distorted trigonal-planar coordination by two nitrogen atoms of different triazenido ligands [Li2–N1 2.013(7) Å; Li2–N4 2.044(7) Å] and the centroid of a η^3 -bonded arene ring [Li2 \cdots C21 2.343(7) Å; Li2 \cdots C22 2.585(7) Å; Li2 \cdots C26 2.605(7) Å]. Notably, the different coordination of the lithium atoms and the N3–Li1–N6 angle of 176.9(6)° allow an alternative description of (**2**)₂ as lithiate complex [Li][Li(N₃Tph)₂]. Steric crowding is manifested in the different conformations of the biphenyl substituents with respect to the central NNN plane. It is reflected by the N–N–C_n1–C_n6 dihedral angles and is best described as being syn/gauche ($n = 1$ and 3) and anti/syn ($n = 5$ and 7).

Unexpectedly, the potassium and cesium triazenides **3** and **4** crystallize as monomeric complexes. They contain symmetrically bonded bidentate triazenide ligands with mean M–N distances of 2.716 and 3.068 Å, respectively. Steric and electronic saturation of the alkali-metal cations is provided by additional metal $\cdots\pi$ -arene contacts to the flanking aryl groups. In **3**, the metal ion interacts with the Trip rings of the biphenyl substituents in a η^6/η^5 fashion with K \cdots C distances in the ranges 3.2948(17)–3.3689(17) Å (C21 \rightarrow C26) and 3.3060(17)–3.4482(18) Å (C41, C42, and C44 \rightarrow C46).¹³ In **4**, the metal $\cdots\pi$ -arene interactions are best described as being η^5/η^5 . The Cs \cdots C distances considered to be bonding are in the ranges 3.541(6)–3.741(6) Å (C21 \rightarrow C25) and

3.664(6)–3.736(6) Å (C41, C42, and C44 \rightarrow C46). For **3** and **4**, the coplanar arrangement of the C₆H₄ rings with the NNN plane and the perpendicular orientation of the Trip substituents result in an unusual T-shaped environment of the metal cations defined by the centroids of the coordinated arene rings and N2 of the triazenido ligand. In **4**, two additional weak agostic-type interactions of 3.784(9) Å (Cs \cdots C222) and 3.811(8) Å (Cs \cdots C462) are observed for the carbon atoms of the *o*-Pr groups. The absence of particular short intermolecular M \cdots C contacts (**3**, K \cdots C > 5.3 Å; **4**, Cs \cdots C > 4.2 Å) supports the monomeric nature for both compounds in the solid state.

¹H NMR studies on C₆D₆ solutions of **3** and **4** indicate that the coplanar conformation of the triazenido ligand and therefore the π encapsulation of the metal cations are retained in solution.¹⁴

Which factors contribute to the different aggregation of **2** vs **3** and **4**? First, the varying interactions of the alkali-metal cations with the flanking aryl substituents need to be considered. Although the strength of the M $\cdots\pi$ -arene interactions normally decreases with increasing radius of M,¹⁵ geometric constraints in the triazenide anion allow close η^6 - π -arene contacts only in the case of the larger metals. In addition, the larger Li–N bond energies and the flexible conformation¹⁶ of the triazenido ligand favor the formation of conventional heteroatom-bridged dimers in **2**. On the other hand, oligomerization of **3** and **4** is prevented by smaller M–N bond energies. The higher tendency of the heavier alkali-metal cations to interact with the pendant aromatic rings may also be viewed in terms of the “hard and soft acids and bases” principle: the soft acids K⁺ and Cs⁺ prefer the soft base arene over the hard base R₂N₃[–].

In summary, we have used a novel sterically crowded, triazenido ligand to stabilize monomeric, unsolvated complexes of the heavier alkali metals potassium and cesium. In contrast to commonly used neutral or anionic multidentate ligands, such as crown ethers, cryptands, or calixarenes, which coordinate via hard σ -donor atoms, steric and electronic saturation of the metal centers in our compounds is mainly achieved by π -arene encapsulation between flanking aryl substituents.

Acknowledgment. We thank the Deutsche Forschungsgemeinschaft (Grant SPP 1166) for financial support.

Supporting Information Available: Details on the preparation and characterization of **1–4** and X-ray data (CIF) for **2–4**. This material is available free of charge via the Internet at <http://pubs.acs.org>.

IC060873F

(9) Moore, D. S.; Robinson, S. D. *Adv. Inorg. Chem. Radiochem.* **1986**, *30*, 1.

(10) Shock-frozen crystals in Paratone N, diffractometer Siemens P3, $T = 173$ K, *SHELXL-97* refinement with all data on F^2 . Crystal data for **2**: yellow block (0.50 \times 0.30 \times 0.15 mm³) from *n*-heptane at 20 °C, C₈₄H₁₀₈Li₂N₆, $M = 1215.64$, triclinic, space group $P\bar{1}$, $a = 13.735(3)$ Å, $b = 15.839(4)$ Å, $c = 19.182(4)$ Å, $\alpha = 79.31(2)^\circ$, $\beta = 85.390(18)^\circ$, $\gamma = 65.750(18)^\circ$, $V = 3738.7(15)$ Å³, $Z = 2$, $\rho_{\text{calc}} = 1.080$ g cm^{–3}, $\mu(\text{Mo K}\alpha) = 0.062$ mm^{–1}, $2\theta_{\text{max}} = 50.0^\circ$, 13 774 ($R_{\text{int}} = 0.055$) collected and 13 170 unique reflections, 887 parameters, 7 restraints, $R_1 = 0.079$ for 6880 reflections with $I > 2\sigma(I)$, $wR_2 = 0.167$ (all data), GOF = 1.191. Crystal data for **3**: deep yellow block (0.75 \times 0.75 \times 0.35 mm³) from benzene at 20 °C, C₄₂H₅₄KN₃, $M = 639.98$, triclinic, space group $P\bar{1}$, $a = 9.4209(14)$ Å, $b = 14.406(3)$ Å, $c = 14.624(3)$ Å, $\alpha = 101.089(16)^\circ$, $\beta = 104.113(13)^\circ$, $\gamma = 91.023(14)^\circ$, $V = 1884.5(6)$ Å³, $Z = 2$, $\rho_{\text{calc}} = 1.128$ g cm^{–3}, $\mu(\text{Mo K}\alpha) = 0.173$ mm^{–1}, $2\theta_{\text{max}} = 55.0^\circ$, 9154 ($R_{\text{int}} = 0.019$) collected and 8625 unique reflections, 441 parameters, 3 restraints, $R_1 = 0.052$ for 7499 reflections with $I > 2\sigma(I)$, $wR_2 = 0.146$ (all data), GOF = 1.028. Crystal data for **4**: yellow plate (0.45 \times 0.22 \times 0.06 mm³) from benzene at 20 °C, C₄₂H₅₄CsN₃, $M = 733.79$, triclinic, space group $P\bar{1}$, $a = 9.538(3)$ Å, $b = 13.232(4)$ Å, $c = 16.727(4)$ Å, $\alpha = 100.37(2)^\circ$, $\beta = 106.21(2)^\circ$, $\gamma = 101.89(2)^\circ$, $V = 1919.2(10)$ Å³, $Z = 2$, $\rho_{\text{calc}} = 1.270$ g cm^{–3}, $\mu(\text{Mo K}\alpha) = 0.996$ mm^{–1}, $2\theta_{\text{max}} = 50.0^\circ$, 7202 ($R_{\text{int}} = 0.059$) collected and 6756 unique reflections, 430 parameters, 2 restraints, $R_1 = 0.063$ for 4543 reflections with $I > 2\sigma(I)$, $wR_2 = 0.139$ (all data), GOF = 1.135. Crystallographic data (excluding structure factors) for the structures reported in this paper have been deposited with the Cambridge Crystallographic Data Centre as supplementary publication nos. CCDC 296485 (**2**), 296487 (**3**), and 607516 (**4**). Copies of the data can be obtained free of charge from CCDC, 12 Union Road, Cambridge CB21EZ, U.K. [fax +(44)-1223-336-033; e-mail deposit@ccdc.cam.ac.uk].

(11) Gantzel, P.; Walsh, P. J. *Inorg. Chem.* **1998**, *37*, 3450.

(12) Cole, M. L.; Davies, A. J.; Jones, C.; Junk, P. C. *New J. Chem.* **2005**, *29*, 1404 and further references cited therein.

(13) The assignment of the hapticity of the metal– π -arene interactions in compounds **3** and **4** is based on the evaluation of the M–centroid distances and the angle between the M–centroid vector and the normal of the arene plane (see the Supporting Information).

(14) The chemical shift for the 6H atom in the 2-Trip-C₆H₄ substituents is very sensitive to conformational changes (see the Supporting Information). A planar conformation (N–N–C1–C6 \approx 0) correlates with a low-field shift [δ 8.38 (**3**) and 8.47 (**4**)], whereas the corresponding signal for **2** is observed at much higher field (δ 6.60).

(15) Nicholas, J. B.; Hay, B. P.; Dixon, D. A. *J. Phys. Chem. A* **1999**, *103*, 1394.

(16) Density functional theory calculations (see the Supporting Information) for different conformers of deprotonated ligand **1** reveal that the syn/anti conformer is destabilized with respect to the syn/syn form by 19.3 kJ/mol.